

Crossover between Integer and Fractional Vortex Lattices in Coherently Coupled Two-Component Bose-Einstein Condensates

Mattia Cipriani^{1,2} and Muneto Nitta³

¹*Department of Physics “E. Fermi”, University of Pisa, Largo Bruno Pontecorvo 3, 56127 Pisa, Italy*

²*Istituto Nazionale di Fisica Nucleare-Sezione di Pisa, Largo Bruno Pontecorvo 3, 56127 Pisa, Italy*

³*Department of Physics, and Research and Education Center for Natural Sciences, Keio University, 4-1-1 Hiyoshi, Yokohama, Kanagawa 223-8521, Japan*

(Received 22 March 2013; published 21 October 2013)

We study the effects of the internal coherent (Rabi) coupling in vortex lattices in two-component BECs under rotation. We find how the vortex lattices without the Rabi coupling known before are connected to the Abrikosov lattice of integer vortices with increasing the Rabi coupling. We find that (1) for small Rabi couplings, fractional vortices in a triangular or square lattice for small or large intercomponent coupling constitute hexamers or tetramers, namely multidimer bound states made of six or four vortices, respectively, (2) these bound states are broken into a set of dimers at intermediate Rabi couplings, and (3) vortices change their partners in various ways depending on the intercomponent coupling, to organize themselves for constituting the Abrikosov lattice of integer vortices at strong Rabi couplings.

DOI: [10.1103/PhysRevLett.111.170401](https://doi.org/10.1103/PhysRevLett.111.170401)

PACS numbers: 05.30.Jp, 03.75.Lm, 03.75.Mn

Multicomponent condensations are one of growing topics in condensed matter physics such as exotic superconductors, superfluid ^3He , multicomponent or spinor Bose-Einstein condensates (BECs) of ultracold atomic gases, exciton-polariton condensates, nonlinear optics, and nonlinear sciences. They also appear in high energy physics and astrophysics such as hadronic matter composed of neutron and proton Cooper pairs relevant for cores of neutron stars, and quark matter composed of diquark condensates consisting of quark Cooper pairs which might be present at higher density. One of the new common features of these systems is the existence of exotic vortices created by rotating superfluids or BECs or by applying a magnetic field on superconductors. There exist different vortices winding around different condensates in general. Their quantized circulations for superfluids or BECs and fluxes for superconductors are not integer valued anymore but are rational or fractional in general, as found in various systems: superfluid ^3He [1,2], p -wave superconductors [1,3–5], multigap superconductors [6,7], spinor BECs [8,9], multicomponent BECs [10–19], exciton-polariton condensates [20,21], nonlinear optics [22], and color superconductors as quark matter [23].

Among various condensed matter systems admitting vortices, BECs of ultracold atomic gases provide a particularly ideal system for examining properties of vortices both theoretically and experimentally [24]. Theoretically, BECs can be quantitatively well described in the mean-field theory, i.e., the Gross-Pitaevskii equation. On the other hand, BECs are quite flexible and controllable systems experimentally, because the atomic interaction is tunable through a Feshbach resonance [25] and the condensates can be visualized directly by optical techniques. Two-component BECs have been realized by

using the mixture of atoms with two hyperfine states of ^{87}Rb [26] or the mixture of two different species of atoms [27–29].

One of fascinating features of fractional vortices is the possibility of various structures of vortex lattices, as found in a vortex phase diagram in two-component BECs [11–15]. When the intercomponent coupling is increased, one obtains from an Abrikosov’s triangular lattice of fractional vortices to a square lattice of fractional vortices [11–13], and a vortex sheet [17]. One may expect a similar phase diagram in exotic superconductors if the rotation speed is replaced with an applied magnetic field. However, for multigap superconductors, the existence of a Josephson coupling between different condensates is inevitable. While this term provides a gap to the Leggett mode corresponding to the phase difference between two condensates, it has been predicted in Refs. [6,7] that it also binds fractional vortices winding around two different components by a sine-Gordon kink [30,31], resulting in a two-vortex molecule, a *dimer*. However, such a molecule structure has not yet been observed in exotic superconductors except for indirect evidences [32]. In two-component BECs of atoms with two hyperfine states such as ^{87}Rb [26], two condensates can be coherently coupled by introducing a Rabi oscillation, which gives the same interaction as the Josephson coupling in superconductors. In fact, with the Rabi couplings, vortices winding around two (or more) different condensates are found to constitute a dimer [13,16] (or a trimer [19]), connected by one (or more) sine-Gordon kink(s) [10]. Similar objects were discussed in spinor BECs [33]. The molecule structures are more accessible in BECs than superconductors because of stronger repulsion between two kinds of vortices and tunable atomic interactions in experiments in BECs. However,

effects on this term were not studied in the vortex phase diagram of two-component BECs.

The purpose of this Letter is to systematically study effects of the Rabi coupling in vortex lattices in two-component BECs under rotation. In the limit of a strong Rabi coupling, each vortex molecule is tightly bound to become an integer vortex, where one can expect the usual Abrikosov lattice of integer vortices. The effects of the coherent coupling were simulated in [34] for an atomic-molecular BEC mixture. However, the richer vortex lattice structure in atomic two-component BECs gives rise to a wider variety of configurations, as shown below. A quite nontrivial question is how the vortex lattices without the Rabi coupling known before are deformed into the integer Abrikosov lattice when the Rabi coupling is gradually increased. We find various new structures of vortex lattices and new phenomena of vortices, i.e., a bound state of multiple dimers bound by an intermolecular force and exchanging partners among multiple multidimer bound states analogous to chemical reactions. For small Rabi couplings, fractional vortices in triangular or square lattice constitute vortex hexamers or tetramers, respectively. With increasing the Rabi coupling, they are broken into a set of dimers. Then, they exchange their partners to organize themselves to prepare for becoming the Abrikosov lattice of integer vortices.

The energy functional of the Gross-Pitaevskii equations for the rotating BECs subject to a trapping harmonic potential can be written as:

$$E = \int d^3r \left\{ \sum_{\alpha=1,2} \Psi_{\alpha}^* \left[\frac{1}{2} \left(\frac{1}{i} \nabla - \Omega \hat{z} \times \mathbf{r} \right)^2 + \frac{r^2}{2} (1 - \Omega^2) - \mu_{\alpha} \right] \Psi_{\alpha} + \frac{1}{2} g_1 |\Psi_1|^4 + \frac{1}{2} g_2 |\Psi_2|^4 + g_{12} |\Psi_1|^2 |\Psi_2|^2 \right\} \quad (1)$$

where the derivatives include (r, θ) coordinates. We measure distances and energies in terms of $b_{ho} = \sqrt{\hbar/m\omega}$ and $\hbar\omega$, respectively, where m is the mass of the atoms and ω is the frequency of the trapping harmonic potential. We consider $g_1 = g_2 = g$.

The phase diagram of the vortex lattice forming in the condensate was studied in [11,12] and a rich variety of lattices was found. The structure of the two component lattice depends on the sign and on the magnitude of g_{12} , the coupling constant of the intercomponent interactions.

When $g_{12}/g = \delta < 0$, the vortices of different components are attracted and are combined into integer vortices. Because of repulsion among them, they organize in a triangular lattice. If $\delta > 0$, depending on the value of δ and Ω , vortices in each component organize in the triangular lattice, the square lattice, or the vortex sheet. When $\delta = 0$ the vortices of each component are organized in an Abrikosov lattice, but the vortices of different components are decoupled. If δ is increased, the intercomponent interaction

results in a repulsive force between the vortices of different components [14,18] and the two-component lattice has a hexagonal structure. When δ is increased further the unitary cell of the single component lattice is changed from a triangle to a square. The value of δ for which the lattice reorganizes depends on rotation speed. If $\delta > 1$, phase separation occurs and vortex sheets appear [17].

We now want to systematically study the effect of an internal coherent coupling on the vortex lattice. When the two different components are atoms with different hyperfine spin states, the coherent coupling can be achieved by Rabi oscillations. This results in the formation of a two-vortex molecule, namely a dimer.

The potential induced by Rabi oscillations has the form

$$V_R = - \int d^3r \omega_R (\Psi_1^* \Psi_2 + \Psi_2^* \Psi_1). \quad (2)$$

This interaction couples the atoms of the two components via the relative phase of the order parameters. We expect the interplay between the Rabi interaction and the atom-atom interaction triggered by g_{12} to be fundamental for the vortex lattice structure. Then we consider the ratio ω_R/δ as the relevant quantity.

We first reproduced the results of [12] by numerically minimizing the free energy (1). They are reported on the horizontal axis of Fig. 1. We minimize the free energy (1) by the nonlinear conjugate gradient method (the imaginary time propagation) in the FreeFem++ package. We calculate the ground state of the system with $\omega_R > 0$ by minimizing the energy functional (1) with (2) added. We use the converged lattice solution obtained with $\omega_R = 0$ as the starting-point configuration and then we increase the Rabi frequency by steps $\Delta\omega_R = \delta/20$. We then take the results of the converged calculation obtained for some value of ω_R as the initial configuration for the next step. By using this ‘‘adiabatic’’ evolution method we are confident that we always obtain the true ground state for the

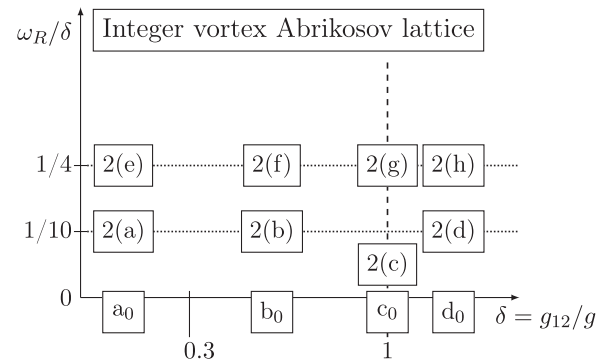


FIG. 1. The vortex lattice phase diagram. a_0 , b_0 , c_0 , d_0 indicate the lattices found in [12]. a_0 corresponds to the triangular lattice, b_0 to the square lattice, and d_0 to the vortex sheet, while c_0 represents the configuration staying at the boundary between lattice and vortex sheet regions. The others are the different configurations explained in the text. The labels refer to the pictures of Fig. 2.

vortex lattice. We cross-checked our results by starting from the converged solution with $\delta = 0$ and moving in the phase diagram along horizontal lines, with steps of $\Delta\delta = 0.1$, keeping the ratio ω_R/δ fixed. We report the results in the Supplemental Material [35]. In all the numerical simulations we take $g = 1$, $\Omega = 0.98$, and $\mu_1 = \mu_2 = 4.5$. The number of atoms is $N_1 = N_2 = N \sim 10^3$, while the value of the healing length $\xi \sim 0.3b_{ho}$. The ground state configurations obtained are schematically reported in Fig. 1. For simplicity, we reported labels for the various configurations which we explain below.

We find that for $\omega_R/\delta \lesssim 1/10$ multidimer bound states appear. When δ takes values corresponding to triangular lattices $0 < \delta \lesssim 0.3$, the system exhibits vortex hexamers connected by domain walls, as shown in Fig. 2(a); if δ is

within the square lattice range $0.3 \lesssim \delta \lesssim 1$, each bound state is composed of four vortices making up tetramers, as shown in Fig. 2(b); when $\delta = 1$ slanted tetramers appear, as shown in Fig. 2(c). This behavior is signaled by the form of the Rabi energy, whose maxima lie between a group of vortices. When the tension of the neighboring domain wall and anti-domain wall is small enough they can bend toward each other and constitute a bound state, because of the attraction between them. The structure of the lattice is schematically reported in the rightmost panels of Figs. 2(a)–2(c). However, these bound states are metastable and when $1/10 \lesssim \omega_R/\delta \lesssim 1/4$ they split into dimers, as in Figs. 2(e)–2(g). The phase separation for $\delta > 1$ prevents the formation of multidimer bound states and only single dimers are formed even for higher values of ω_R/δ , as shown in

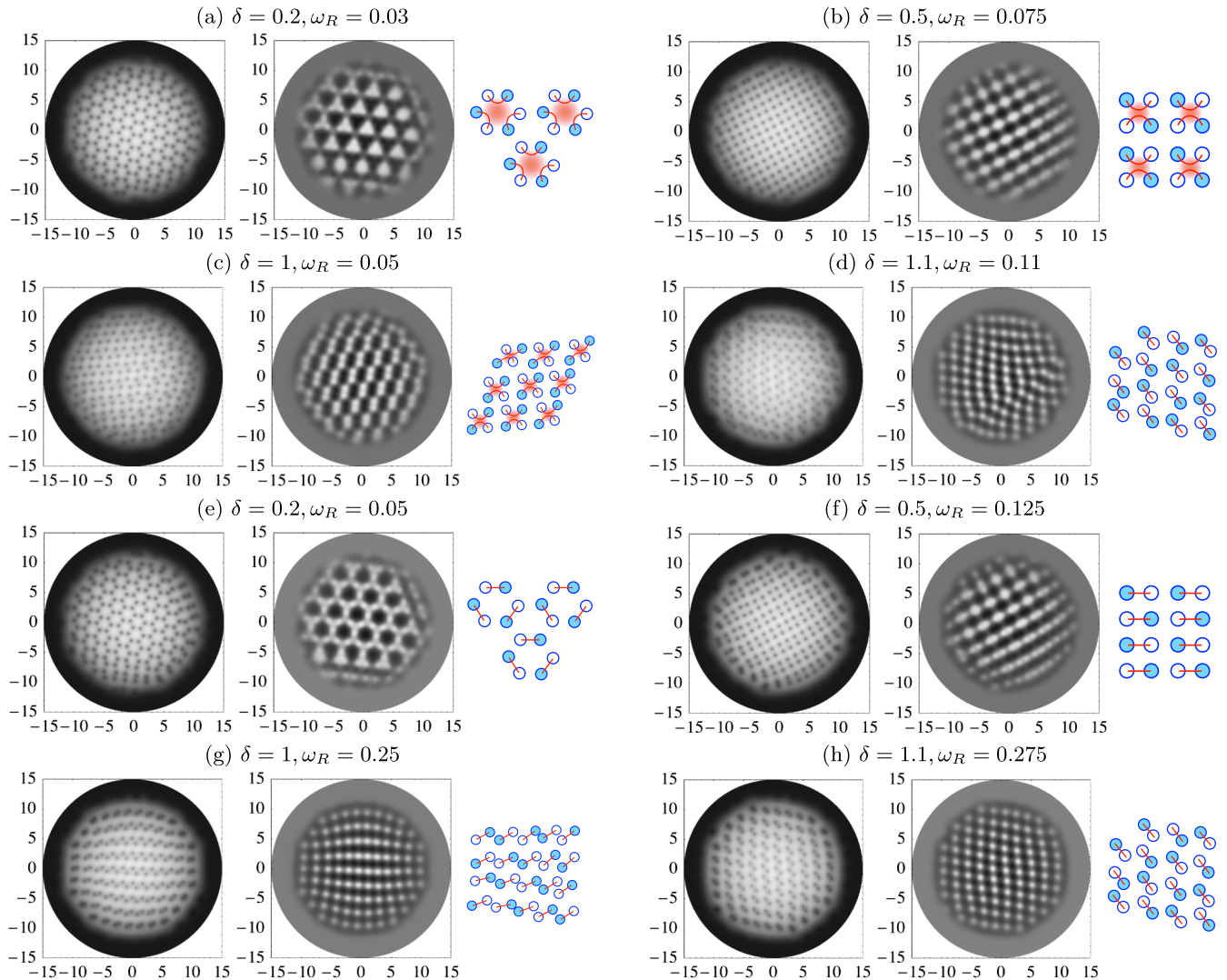


FIG. 2 (color online). In all subfigures the left panel is a plot of the density profile of the condensate, $n = |\Psi_1|^2 + |\Psi_2|^2$ (dark grey dots are vortices of the first or the second component), the middle panel is a plot of the Rabi energy in Eq. (2) (white is positive, identified with domain walls), and the right panel is a schematic drawing of the lattice structure. The domain walls joining vortices are depicted as red lines and the vortices in the first and in the second component are distinguished by empty or filled circles. The values of the parameters δ and ω_R are shown for each case. The lattice defect in (d) appears just by chance and in fact it resolves with increasing ω_R , as can be seen in subfigure (h). Panels (e)–(g) show the same cases of (a)–(c) with higher ω_R . To visualize the domain walls, the plots of the phase difference between the two condensates are given in the Supplemental Material [35].

Figs. 2(d) and 2(h). This happens because, for $\delta > 1$, even with very small ω_R , there are no dimers whose domain walls are so close to bend and form multidimer molecules. This can be seen from Figs. 2(d) and 2(h).

When ω_R increases further, the lattice modifies drastically. The reason for this modification is that for large values of ω_R the dimers are undistinguishable from integer vortices, in which the positions of the vortices of the first and the second components coincide. Integer vortices repel each other and are organized in an Abrikosov lattice. However, to reach the Abrikosov configuration, the various lattices of fractional vortices must be deeply modified. This modification is achieved when $1/4 \lesssim \omega_R/\delta \lesssim 1/3$. The vortices change their partners.

We were able to find the elementary patterns of rearrangement, shown in Fig. 3. In the rightmost panel of each subfigure schematic, representations of the process of partner changing are reported. We indicate with round solid boxes the dimers left unchanged, while the dashed boxes represent the formation of new dimers. When $0 < \delta \lesssim 0.3$ the lattice is triangular for $\omega_R/\delta \lesssim 1/4$, but when ω_R is increased the domain walls connecting vortices in dimers can break and reconnect as depicted in Fig. 3(a). The partner changing process can be realized along three different directions. This is due to the discrete rotational symmetry of the two-component hexagonal vortex lattice appearing when $\delta < 0.3$. All these possibilities are realized in general. When the lattice structure is very symmetric, as in the case of Fig. 3(a), the lattice is divided into three domains separated by a domain wall junction, as can be seen from the picture in the left panel where the density profile of the condensate is shown. In general, configurations with more defects are obtained, as shown in the Supplemental Material [35].

If $0.3 \lesssim \delta < 1$, the vortices can change partners in two different ways, as shown in Figs. 3(b) and 3(c). The rightmost panels represent the patterns of the partner changing processes, with the same conventions as of Fig. 3(a). As can be seen from the schematic diagram in Fig. 3(b), four vortices forming a square cell change their partner, while links in the adjacent square cell are kept unchanged. The situation is different in Fig. 3(c), where vortices change their partner in alternating rows. The disposition of the dimers depicted in the bottom rightmost panel of Fig. 3(c) is similar to that of Fig. 2(h). However, for $\delta > 1$ the free energy is minimized when vortices of the same component are close to each other, forming vortex sheets. Instead in the case of Fig. 3(c), the lower energy is achieved when vortices belonging to the same component are well separated. This explains why in 2(h) vortices of the same component of adjacent dimers are close to each other, while in 3(c) they are not. The rearrangement of Fig. 3(b) is difficult to obtain in the whole lattice; nevertheless, limited portions of the lattice always show this pattern, in the indicated parameter ranges, as reported in the Supplemental Material [35]. The pattern of Fig. 3(c) is frequently obtained when δ is in the square lattice range.

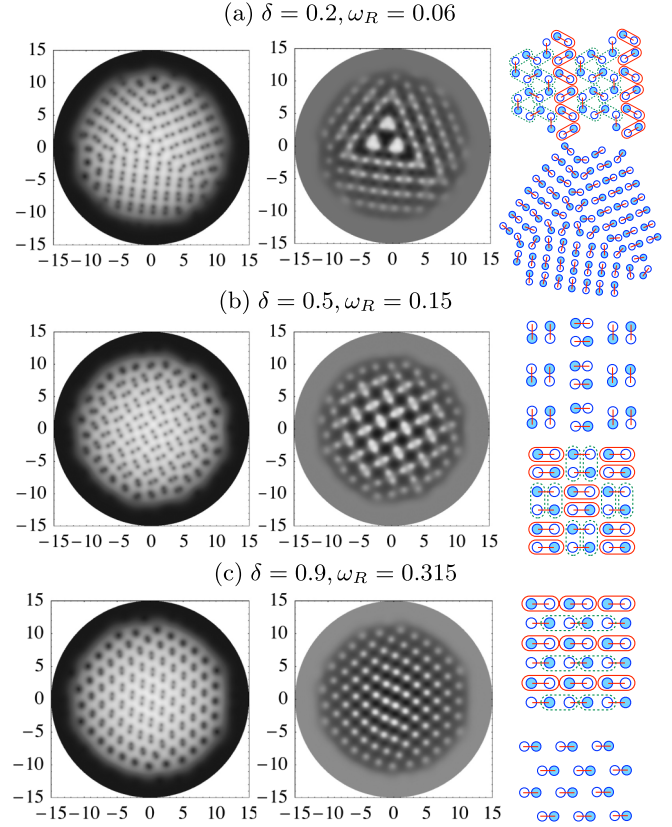


FIG. 3 (color online). (a–c) The different partner changing patterns that we have identified. The left panel in each subfigure shows the plot of the density profile of the condensate $n = |\Psi_1|^2 + |\Psi_2|^2$ (dark grey dots are vortices of the first or the second component) and the middle panel shows the Rabi energy in Eq. (2) (white is positive, identified as domain walls). Schematic reproductions of the modifications on the dimers and of the lattice itself after the partner changing took place are shown in the right panel in each row. The domain walls joining vortices are depicted as red lines and the vortices in the first or in the second component are distinguished by empty or filled circles. The domain walls are broken and reconnected to be new sets of dimers indicated by the dashed round boxes; the dimers indicated by solid round boxes are instead kept unchanged. To visualize the domain walls, the plots of the phase difference between the two condensates are given in the Supplemental Material [35].

In conclusion, we have found a rich variety of lattices which can appear in two-component BECs where internal coherent coupling is induced. We introduced the interaction via Rabi oscillations and studied systematically its effect on the vortex lattice, increasing gradually the frequency ω_R from $\omega_R = 0$. The vortex lattice is reorganized when ω_R is increased up to high values in order to reach the triangular lattice configuration where all dimers become integer vortices. During this process multidimer bound states are formed and vortices can exchange partners in different ways, depending on the form of the fractional vortex lattice. The patterns of the exotic vortex lattices which we have found in this Letter can be easily distinguished from the usual triangular or square lattice from observations for instance by the time of flight.

M. C. thanks the Department of Physics at Hiyoshi, Keio University, for warm hospitality in the beginning of this project. M. N. thanks INFN, Pisa, for partial support and hospitality while this work was done. We thank Kenichi Kasamatsu and Yasumoto Tanaka for useful comments. The numerical calculations were performed on the INFN CSN4 cluster located in Pisa. The work of M. N. is supported in part by KAKENHI (No. 23740198, No. 23103515, No. 25400268, and No. 25103720).

-
- [1] M. M. Salomaa and G. E. Volovik, *Phys. Rev. Lett.* **55**, 1184 (1985); *Rev. Mod. Phys.* **59**, 533 (1987).
- [2] G. E. Volovik, *The Universe in a Helium Droplet* (Clarendon Press, Oxford, 2003).
- [3] D. A. Ivanov, *Phys. Rev. Lett.* **86**, 268 (2001).
- [4] S. B. Chung, H. Bluhm, and E.-A. Kim, *Phys. Rev. Lett.* **99**, 197002 (2007); S. B. Chung and S. A. Kivelson, *Phys. Rev. B* **82**, 214512 (2010).
- [5] J. Jang, D. G. Ferguson, V. Vakaryuk, R. Budakian, S. B. Chung, P. M. Goldbart, and Y. Maeno, *Science* **331**, 186 (2011).
- [6] E. Babaev, *Phys. Rev. Lett.* **89**, 067001 (2002); E. Babaev, A. Sudbo, and N. W. Ashcroft, *Nature (London)* **431**, 666 (2004); J. Smiseth, E. Smorgrav, E. Babaev, and A. Sudbo, *Phys. Rev. B* **71**, 214509 (2005); E. Babaev and N. W. Ashcroft, *Nat. Phys.* **3**, 530 (2007).
- [7] J. Goryo, S. Soma, and H. Matsukawa, *Europhys. Lett.* **80**, 17 002 (2007).
- [8] T.-L. Ho, *Phys. Rev. Lett.* **81**, 742 (1998); T. Ohmi and K. Machida, *J. Phys. Soc. Jpn.* **67**, 1822 (1998).
- [9] G. W. Semenoff and F. Zhou, *Phys. Rev. Lett.* **98**, 100401 (2007); M. Kobayashi, Y. Kawaguchi, M. Nitta, and M. Ueda, *Phys. Rev. Lett.* **103**, 115301 (2009).
- [10] D. T. Son and M. A. Stephanov, *Phys. Rev. A* **65**, 063621 (2002).
- [11] E. J. Mueller and T.-L. Ho, *Phys. Rev. Lett.* **88**, 180403 (2002).
- [12] K. Kasamatsu, M. Tsubota, and M. Ueda, *Phys. Rev. Lett.* **91**, 150406 (2003).
- [13] K. Kasamatsu, M. Tsubota, and M. Ueda, *Int. J. Mod. Phys. B* **19**, 1835 (2005).
- [14] A. Aftalion, P. Mason, and J. Wei, *Phys. Rev. A* **85**, 033614 (2012).
- [15] P. Kuopanportti, J. A. M. Huhtamäki, and M. Möttönen, *Phys. Rev. A* **85**, 043613 (2012).
- [16] K. Kasamatsu, M. Tsubota, and M. Ueda, *Phys. Rev. Lett.* **93**, 250406 (2004).
- [17] K. Kasamatsu and M. Tsubota, *Phys. Rev. A* **79**, 023606 (2009).
- [18] M. Eto, K. Kasamatsu, M. Nitta, H. Takeuchi, and M. Tsubota, *Phys. Rev. A* **83**, 063603 (2011).
- [19] M. Eto and M. Nitta, *Phys. Rev. A* **85**, 053645 (2012).
- [20] Y. G. Rubo, *Phys. Rev. Lett.* **99**, 106401 (2007); K. G. Lagoudakis, T. Ostatnický, A. V. Kavokin, Y. G. Rubo, R. Andre, and B. Deveaud-Pledran, *Science* **326**, 974 (2009); Y. G. Rubo, [arXiv:1209.6538](https://arxiv.org/abs/1209.6538); G. Roumpos, M. D. Fraser, A. Löffler, S. Höfling, A. Forchel, and Y. Yamamoto, *Nat. Phys.* **7**, 129 (2011).
- [21] J. Keeling and N. G. Berloff, *Phys. Rev. Lett.* **100**, 250401 (2008); M. O. Borgh, G. Franchetti, J. Keeling, and N. G. Berloff, *Phys. Rev. B* **86**, 035307 (2012).
- [22] L. M. Pismen, *Phys. Rev. Lett.* **72**, 2557 (1994); L. M. Pismen, *Physica (Amsterdam) D* **73**, 244 (1994); I. S. Aranson and L. M. Pismen, *Phys. Rev. Lett.* **84**, 634 (2000); L. M. Pismen, *Vortices in Nonlinear Fields: From Liquid Crystals to Superfluids, from Non-Equilibrium Patterns to Cosmic Strings* (Oxford University Press, New York, 1999).
- [23] A. P. Balachandran, S. Dugal, and T. Matsuura, *Phys. Rev. D* **73**, 074009 (2006); E. Nakano, M. Nitta, and T. Matsuura, *Phys. Rev. D* **78**, 045002 (2008); M. Eto and M. Nitta, *Phys. Rev. D* **80**, 125007 (2009); M. Eto, E. Nakano, and M. Nitta, *Phys. Rev. D* **80**, 125011 (2009); M. Eto, M. Nitta, and N. Yamamoto, *Phys. Rev. Lett.* **104**, 161601 (2010).
- [24] C. J. Pethick and H. Smith, *Bose-Einstein Condensation in Dilute Gases* (Cambridge University Press, Cambridge, England, 2008), 2nd ed.
- [25] C. Chin, R. Grimm, P. Julienne, and E. Tiesinga, *Rev. Mod. Phys.* **82**, 1225 (2010).
- [26] C. J. Myatt, E. A. Burt, R. W. Ghrist, E. A. Cornell, and C. E. Wieman, *Phys. Rev. Lett.* **78**, 586 (1997); D. S. Hall, M. R. Matthews, J. R. Ensher, C. E. Wieman, and E. A. Cornell, *Phys. Rev. Lett.* **81**, 1539 (1998); K. M. Mertes, J. W. Merrill, R. Carretero-González, D. J. Frantzeskakis, P. G. Kevrekidis, and D. S. Hall, *Phys. Rev. Lett.* **99**, 190402 (2007); S. Tojo, Y. Taguchi, Y. Masuyama, T. Hayashi, H. Saito, and T. Hirano, *Phys. Rev. A* **82**, 033609 (2010).
- [27] G. Modugno, M. Modugno, F. Riboli, G. Roati, and M. Inguscio, *Phys. Rev. Lett.* **89**, 190404 (2002); G. Thalhammer, G. Barontini, L. De Sarlo, J. Catani, F. Minardi, and M. Inguscio, *Phys. Rev. Lett.* **100**, 210402 (2008).
- [28] S. B. Papp, J. M. Pino, and C. E. Wieman, *Phys. Rev. Lett.* **101**, 040402 (2008).
- [29] D. J. McCarron, H. W. Cho, D. L. Jenkin, M. P. Köppinger, and S. L. Cornish, *Phys. Rev. A* **84**, 011603(R) (2011).
- [30] Y. Tanaka, *J. Phys. Soc. Jpn.* **70**, 2844 (2001); *Phys. Rev. Lett.* **88**, 017002 (2001).
- [31] A. Gurevich and V. M. Vinokur, *Phys. Rev. Lett.* **90**, 047004 (2003).
- [32] A. Crisan, Y. Tanaka, D. D. Shivagan, A. Iyo, L. Cosereanu, K. Tokiwa, and T. Watanabe, *Jpn. J. Appl. Phys.* **46**, L451 (2007); Y. Tanaka, A. Crisan, D. D. Shivagan, A. Iyo, K. Tokiwa, and T. Watanabe, *Jpn. J. Appl. Phys.* **46**, 134 (2007); A. Crisan, A. Iyo, Y. Tanaka, H. Matsuhata, D. Shivagan, P. Shirage, K. Tokiwa, T. Watanabe, T. Button, and J. Abell, *Phys. Rev. B* **77**, 144518 (2008); J. Guikema, H. Bluhm, D. Bonn, R. Liang, W. Hardy, and K. Moler, *Phys. Rev. B* **77**, 104515 (2008); L. Luan, O. Auslaender, D. Bonn, R. Liang, W. Hardy, and K. Moler, *Phys. Rev. B* **79**, 214530 (2009).
- [33] A. M. Turner and E. Demler, *Phys. Rev. B* **79**, 214522 (2009).
- [34] S. J. Woo, Q. Han Park, and N. P. Bigelow, *Phys. Rev. Lett.* **100**, 120403 (2008).
- [35] See Supplemental Material at <http://link.aps.org/supplemental/10.1103/PhysRevLett.111.170401> for phase difference plots of the configurations of Figs. 2 and 3 and results of additional calculations needed to confirm the results of this work.